

N70-28239

TM-70-1011-3

TECHNICAL MEMORANDUM

**A PHYSICAL MODEL OF APOLLO
OXYGEN RELEASES**

**CASE FILE
COPY**

Bellcomm

BELLCOMM, INC.

955 L'ENFANT PLAZA NORTH, S.W., WASHINGTON, D.C. 20024

COVER SHEET FOR TECHNICAL MEMORANDUM**TITLE-** A Physical Model of Apollo Oxygen
Releases**TM-** 70-1011-3**FILING CASE NO(S)-** 340**DATE-** April 29, 1970**AUTHOR(S)-** A. C. Buffalano**FILING SUBJECT(S)**
(ASSIGNED BY AUTHOR(S))-**ABSTRACT**

During the Apollo 8 lunar flight, 3300 kilograms of liquid oxygen were released from the S-IVB 45,000 kilometers from the earth during a normal mission operation. The oxygen froze immediately forming a large (500 km) cloud of small particles. The cloud was photographed by the Smithsonian Astrophysical Observatory's satellite tracking station in Spain over a 90 minute period.

We have reduced this photometric data using a simple collisionless model for the expansion and have deduced the following parameters. The particles which are responsible for the scattering have a bulk velocity of 1.4×10^4 cm/sec and a thermal velocity of $.3 \times 10^4$ cm/sec. While we are unable at this time to estimate the radius of the scatterers with any confidence, we did establish a lower bound of one micron.

SEE REVERSE SIDE FOR DISTRIBUTION LIST

DISTRIBUTIONCOMPLETE MEMORANDUM TO

CORRESPONDENCE FILES:

OFFICIAL FILE COPY

plus one white copy for each
additional case referenced

TECHNICAL LIBRARY (4)

NASA Headquarters

R. O. Aller/MF
W. O. Armstrong/MTX
P. E. Culbertson/MT
M. Dubin/SG
E. W. Hall/MTG
H. Hall/MT-2
R. W. Johnson/MF
T. A. Keegan/MA-2
C. M. Lee/MA
R. L. Lohman/MF
D. R. Lord/MF
T. H. McMullen/MA
L. Roberts/OART-M (2)
A. D. Schnyer/MTE
M. G. Waugh/MT-1
J. W. Wild/MTE

Manned Spacecraft Center

C. E. Allday/FM3
C. L. Dumis/FC3
M. P. Frank/FC
S. H. Gardner/CF34
G. D. Griffin/FC
T. W. Holloway/CF34
E. F. Kranz/FC
R. W. Kubicki/PD
D. L. Lind/CB
J. P. Mayer/FM
J. W. O'Neill/CF34
H. A. Rotter/EC3
F. H. Samonski/EC3
J. H. Sasser/TJ
G. Shinkle/CF32
W. N. Teague/CF32

Marshall Space Flight Center

R. Beaman/PM-SAT-E
J. Dozier/S&E-SSLX
J. P. Lindberg/S&E-AERO-M

COMPLETE MEMORANDUM TOMarshall Space Flight Center

M. Naumcheff/PM-MO-O
J. M. Rives/PM-MO-R
F. A. Speer/PM-MO-MGR
G. Wittenstein/S&E-AERO-MFT

Goddard Space Flight Center

J. Barsky/832
G. P. Bonner/TG4
O. M. Covington/800
J. R. Demeo/832
B. Dixon/832
R. P. Kovar/TG4
R. Strafella/832
L. Woldorff/832

Bellcomm, Inc.

G. M. Anderson
D. J. Belz
A. P. Boysen, Jr.
J. O. Cappellari, Jr.
D. A. Corey
C. L. Davis
D. A. DeGraaf
F. El-Baz
D. R. Hagner
N. W. Hinners
W. W. Hough
B. T. Howard
D. B. James
J. Kranton
H. S. London
W. I. McLaughlin
J. Z. Menard
G. T. Orrok
I. M. Ross
W. Strack
W. B. Thompson
J. W. Timko
T. C. Tweedie
R. L. Wagner
J. E. Waldo
M. P. Wilson
D. B. Wood

All Members Division 101
Department 1024 File
Central File
Library

SUBJECT: A Physical Model of Apollo Oxygen
Releases - Case 340

DATE: April 29, 1970

FROM: A. C. Buffalano

TM-70-1011-3

TECHNICAL MEMORANDUM

1.0 INTRODUCTION

During the Apollo lunar missions, the upper stage of the Saturn launch vehicle, the S-IVB, propels the Apollo spacecraft out of earth orbit and on to a lunar trajectory. The spent S-IVB then separates from the spacecraft, turns perpendicular to the flight path, and is placed on a trajectory which carries it around the trailing limb of the moon and into solar orbit. The thrust for this final maneuver is provided by thousands of kilograms of unburned liquid oxygen which are blown out through the S-IVB's engine. Figure 1 is one in a series of 150 photographs of such a release taken by the Smithsonian Astrophysical Observatory's satellite tracking station in San Fernando, Spain on December 21, 1969 during the Apollo 8 mission [Lundquist 1969, Vaughan 1969]. During the period of photography San Fernando was in darkness and the cloud was illuminated by the sun. Light scattered from the solid oxygen particles produced the large fan shaped object marked (1). Object (2) is the S-IVB and the 'wings' around it are small clouds of hydrogen which is also venting. Object (3) is the spacecraft on its way to the moon [Grobman 1969]. The cloud is about 45,000 kilometers from the earth.

These photographs provide an opportunity to study materials released in space. This is important for two reasons. First, quantifying the dominant physical processes will permit us to build a better model of the environment of future orbiting observatories [Newkirk 1967, Kovar 1969, Grobman 1969, Buffalano 1969]; and second, photoreduction can provide estimates of the optical properties of materials which may be found in interstellar and interplanetary grains [Plummer 1969, Wickramasinghe 1967, Krishna Swamy 1968, 1969].

2.0 PHYSICAL MODEL

When the S-IVB vents, 3300 kilograms of liquid oxygen escape in 150 seconds [Vaughan 1969] and freeze immediately. Since the bulk velocity is approximately 10^4 cm/sec, we will begin by assuming that at time zero all the mass is contained inside a cone of half angle θ_c and length R_c (~ 15 kilometers). Next, we will show that this volume is so large that the system will be collisionless and optically thin at visual wavelengths.

The mean free-path for collisions between particles of radius 'a' and density ρ (~ 1 gm/cm³) in an ensemble of total mass M_t contained in the cone is roughly

$$\text{mfp} \sim \frac{\pi a \rho R_c^3 (1 - \cos \theta_c)}{M_t} \quad (1)$$

The system will be collisionless when the mean free-path is larger than the dimension of the system. This is when

$$R_c > [a (1 - \cos \theta_c)]^{-\frac{1}{2}} \text{ kilometers} \quad (2)$$

where 'a' is in microns. We will subsequently suggest that initially

the scattering particles are larger than 1μ and θ_c is about 30° so the system will be collisionless if

$$R_c > 3 \text{ kilometers} \quad (3)$$

Since R_c is 15 kilometers the system is collisionless and optically thin.

The largest force acting on these particles is considered to be radiation pressure [Newkirk 1967]. Since the cloud is illuminated approximately at right angles to the line of sight any cloud drift due to radiation pressure would appear as a movement across the field of view. No such drifting is seen in the photographs so the particles will be assumed to be essentially free from forces. In addition, this allows us to obtain a lower bound on the particle size. The drift displacement is given by

$$\text{Drift} \sim \frac{3 F_\odot t^2}{8 \rho c a} \quad (4)$$

where F_\odot is the solar constant, c is the velocity of light, and the cross section for momentum transfer has been taken to be the geometric cross section. The photographs show that the drift did not exceed 40 kilometers after 90 minutes, so the particles are probably larger than one micron in radius.

In the absence of collisions and forces the time evolution of the particle distribution function is given by the Liouville equation

$$\frac{\partial f}{\partial t} + \mathbf{u} \cdot \nabla f = 0 \quad (5)$$

The solution is well known and states simply that f is constant along particle trajectories

$$f(\underline{x}, \underline{u}, t) = f(\underline{x} - \underline{u}t, \underline{u}, 0) \quad (6)$$

A prescription of the initial condition $f(\underline{x}, \underline{u}, 0)$ is all that is required for a complete description of the system. We suggest that the release may be treated as though all the mass were initially contained inside a cone-shaped region of length R_c (~ 15 kilometers) and half angle θ_c with a Maxwellian velocity distribution function characterized by a single thermal velocity V_t and streaming velocity V_o . The streaming velocity represents the non-random velocity produced in the nozzle and is radial at every point in the cone.

Since particles of many sizes are probably present in the cloud the use of only one streaming velocity contains an important implicit assumption. Either there is little correlation between particle size and streaming velocity or the size distribution of particles is relatively narrow in the size range producing the scattering. The data reduction tends to support the assumption but does not differentiate between these possibilities.

Combining all these assumptions, the particle distribution function can be written

$$f(\underline{x}, \underline{u}, t) = \frac{3M_t \exp \left\{ -V_t^{-2} \left(\{u_r - V_o\}^2 + u_\alpha^2 + u_\beta^2 \right) \right\}}{2 \pi^{5/2} (1 - \cos \theta_c) R_c^3 V_t^3} \quad (7)$$

if $\underline{x} - \underline{u}t$ is inside the cone
 $= 0$, if $\underline{x} - \underline{u}t$ is outside the cone

Here (u_r, u_α, u_β) are the particle velocity components in a cylindrical coordinate system whose pole is in the radial direction at every point inside the cone as shown in Figure 2. The mass density $\rho(r, \theta)$ is obtained at a field point $P = (r \sin \theta, 0, r \cos \theta)$ by integrating f over the velocity space. The integration is most readily performed in the Cartesian space (u_x, u_y, u_z) . Equation 7 shows that f is non-zero only over the part of the \underline{u} space shown in Figure 3. Integration gives

$$\rho\left(\frac{r}{t}, \theta\right) = \frac{M_t H \exp \left\{ -V_t^{-2} \left(\frac{r}{t} - V_o\right)^2 \right\}}{2 \pi^{5/2} t^3 V_t^3} \quad (8)$$

$$\text{where } H = \frac{\int_0^{\theta_c} d\alpha \sin \alpha \int_0^{2\pi} d\beta \exp \left\{ \frac{2rV_o}{tV_t^2} (\sin \theta \cos \beta \sin \alpha + \cos \alpha \cos \theta - 1) \right\}}{1 - \cos \theta_c}$$

and terms of order $\frac{R_c}{V_t t}$ have been dropped. The parameter $\frac{R_c}{V_t t}$ is between .1 and .4 for the data considered and calculations including these terms show that Equation (8) adequately represents the qualitative and quantitative of this model.

The brightness of an optically thin cloud may be estimated as [Van deHulst 1957]

$$\frac{B}{B_\odot} = \Omega_\odot \bar{\sigma} M \quad (9)$$

where Ω_{\odot} is the solid angle subtended by the solar disc, $\bar{\sigma}$ is the total scattering cross section per unit mass, and M is the mass column density. The measure of brightness, B/B_{\odot} , compares the radiance, B , of an extended source to the radiance of the sun, B_{\odot} . Radiance, B , is defined as the amount of energy crossing a unit area of detector in a unit time and coming from a unit solid angle of source. The mass column density is given by

$$M = \int dl \rho(r) \quad (10)$$

and the scattering cross section per unit mass is given by

$$\bar{\sigma} = \frac{3}{4\pi\rho} \frac{\int da g(a) \sigma(a, \phi)}{\int da a^3 g(a)} \quad (11)$$

where $g(a)$ is the size distribution function, l is the distance from the observer to a scatterer (the integration is performed along the line of sight), σ is the particle differential scattering cross section, and ϕ is the angle between the line joining the scatterer and the sun and the line joining the scatterer and the observer. The integration indicated in (10) gives for the relative brightness $\frac{B}{B_{\odot}}$

$$\frac{B}{B_{\odot}} = \frac{\Omega_{\odot} \bar{\sigma} M_t}{2 \pi^{5/2} t^2 V_t^2} \int_{-\infty}^{+\infty} d\left(\frac{l}{V_t t}\right) H \exp \left\{ -V_t^{-2} \left(\frac{r}{t} - V_o\right)^2 \right\} \quad (12)$$

3.0 DATA REDUCTION

The Smithsonian Astrophysical Observatory (SAO) operates a world-wide network of Baker-Nunn satellite tracking cameras. These are modified Super-Schmidt F/1 telescopes consisting of a 31 inch spherical mirror and three corrector elements. The aperture and focal length are both 500 millimeters.

After film has been removed from the camera, a sensitometer exposes a small portion of the film to a light source through a density wedge producing twenty one levels of exposure. The film is then developed at the station and the negatives are sent to the SAO headquarters in Cambridge, Massachusetts. There, the area exposed through the density wedge is passed through a microdensitometer which measures the density of exposed grains for each exposure level. The negatives are then run through the densitometer and grain density is measured as a function of location on the film [Solomon 1967].

A satisfactory absolute calibration of the film has not been made. Analysis of the SAO film is based therefore on the relative brightness B/B_{\max} where B_{\max} is the maximum cloud brightness in a frame. The relative brightness is given by:

$$\frac{B}{B_{\max}} = \frac{10^{0.15(j-j_{\text{sky}})} - 1}{10^{0.15(j_{\max}-j_{\text{sky}})} - 1} \quad (13)$$

where j is the wedge step number corresponding to the measured grain density at an arbitrary point in the cloud, j_{sky} is the wedge step number of the dark sky background, and j_{max} is the wedge step number at the point of maximum brightness in the cloud.

Of the 150 frames taken, eight were chosen for reduction. They are approximately six minutes apart in time and the first was taken twenty minutes after the oxygen was released. Earlier frames were taken during twilight and were not used and later frames did not produce usable images.

The relative cloud brightness was calculated at about 29 points in each frame using (13).

4.0 RESULTS AND CONCLUSIONS

Since the particles are continuously subliming, $\bar{\sigma}M_t$ changes in time. However, because of our assumption that either the size distribution function is peaked for efficient scatterers or there is no size-velocity correlation, $\bar{\sigma}M_t$ does not vary from point to point in the cloud. This permits us to separate the sublimation effects and study the dynamics alone. Equation (12) shows that if the cloud brightness in any frame is normalized using the maximum brightness in that frame, B_{max} , and if B/B_{max} is plotted versus $(x/t, z/t)$, a time independent shape should result. Figures 4 and 5 show that this is the case. Figure 4 is a trace down the center line of the cloud and Figure 5 is a transverse scan of the cloud through the point of maximum brightness. In these figures, data points from the eight frames are shown superimposed.

By choosing various values of θ_c , V_t , and V_o and using them in (12) one can fit the data as shown by the solid line in Figures 4 and 5. This fit was obtained by straightforward trial and error and was chosen because it gave what we consider to be a satisfactory overall reduction of the data. The values obtained by this method, $V_o = 1.4 \times 10^4$ cm/sec and $V_t = .3 \times 10^4$ cm/sec, seem reasonable since the thermal speed of oxygen in the S-IVB tanks is about 3×10^4 cm/sec, and $\theta_c = 30^\circ$ also seems reasonable since it is larger than the engine's opening angle and less than 90° . Of course we do not expect to obtain a detailed fit to the data because we have had to guess at the form of the initial condition and because we neglected terms in $R_c/V_t t$. The addition of more parameters describing the spatial variation of the initial distribution function and its deviation from thermal equilibrium would be required to improve the fit.

The fit is poorest in Figure 5 at the lateral edges of the cloud far from the cone center line and outside the region defined by the cone half angle. This is reasonable since the particles which arrive in this region come from the low probability regions of the initial distribution function and are therefore most sensitive to variations in the initial condition. Furthermore the initial distribution function is really only approximately zero outside the cone. The particles neglected by the approximation are just the ones most likely to end up in these regions of poor fit.

The good overall fit shown in Figures 4 and 5 encourages us to believe that the actual physics of the expansion has been properly modeled and that the deviations can be attributed to an imprecise statement of the initial condition. We hope to corroborate these conclusions and obtain particle size estimates when better photometry is done on future Apollo flights.

ACKNOWLEDGEMENTS

We are deeply indebted to the staff members of the Smithsonian Astrophysical Observatory, particularly Dr. Charles Lundquist and Edward Jentsch.

A. C. Buffalano

A. C. Buffalano

1011-ACB-sh

- Buffalano, A. C., Water and cryogens in space: some physical considerations, Bellcomm Memorandum For File, Sept. 1969. Presented at Symposium on Optical Contamination in Space, Rocky Mountain Section, Optical Society of America, Aspen, Colorado, Aug. 13-15, 1969.
- Grobman, W. D. and A. C. Buffalano, New conclusions concerning the observation of faint sources from a sunlit spacecraft, Planet. Space Sci., 17, 1089, 1969.
- Grobman, W. D., Use of state vectors to identify the CSM and S-IVB in photographs of the Apollo 8 mission, Bellcomm Memorandum for File, March, 1969.
- Kovar, N. S., R. P. Kovar, and G. P. Bonner, Light scattering by manned spacecraft atmospheres, Planet. Space Sci., 17, p. 143, 1969.
- Krishna Swamy, K. S. and N. C. Wickramasinghe, On the temperature of interstellar grains, Monthly Notices of Royal Astronomical Society, 139, 283, 1968.
- Krishna Swamy, K. S. and N. C. Wickramasinghe, Strength of the fundamental bands of ice and solid hydrogen in composite grains, The Observatory, 89, 57, 1969
- Lundquist, C. A., Photometry from Apollo tracking, XII Plenary Meeting of COSPAR, Prague, May 1969.
- Newkirk, G., The optical environment of manned spacecraft, Planet. Space Sci., 15, 1267, 1967.
- Plummer, W. T., Infrared reflectivity of frost and the Venus clouds, J. Geophys. Res., 74, 3331, 1969

BELLCOMM, INC.

Solomon, L. H. , Some results at Baker-Nunn tracking stations,
Smithsonian Astrophysical Observatory Special Report, 244,
1967.

Van deHulst, H. C., Light Scattering by Small Particles,
J. Wiley & Sons, New York, 1957.

Vaughan, O. H., An analysis and discussion of some Apollo 8
mission events as recorded by the Smithsonian Astrophysical
Observatory, submitted for the Apollo 8 Science Rep.,
National Aeronautics and Space Administration Manned
Spacecraft Center, 1969.

Wickramasinghe, N. C. and K. S. Krishna Swamy, Solid hydrogen
coated graphite particles in the interstellar medium,
I., Preprint of the Steward Observatory, University of
Arizona, November 1968, Tucson, Arizona.

Wickramasinghe, N. C., Interstellar Grains, Chapman and Hall,
1957.

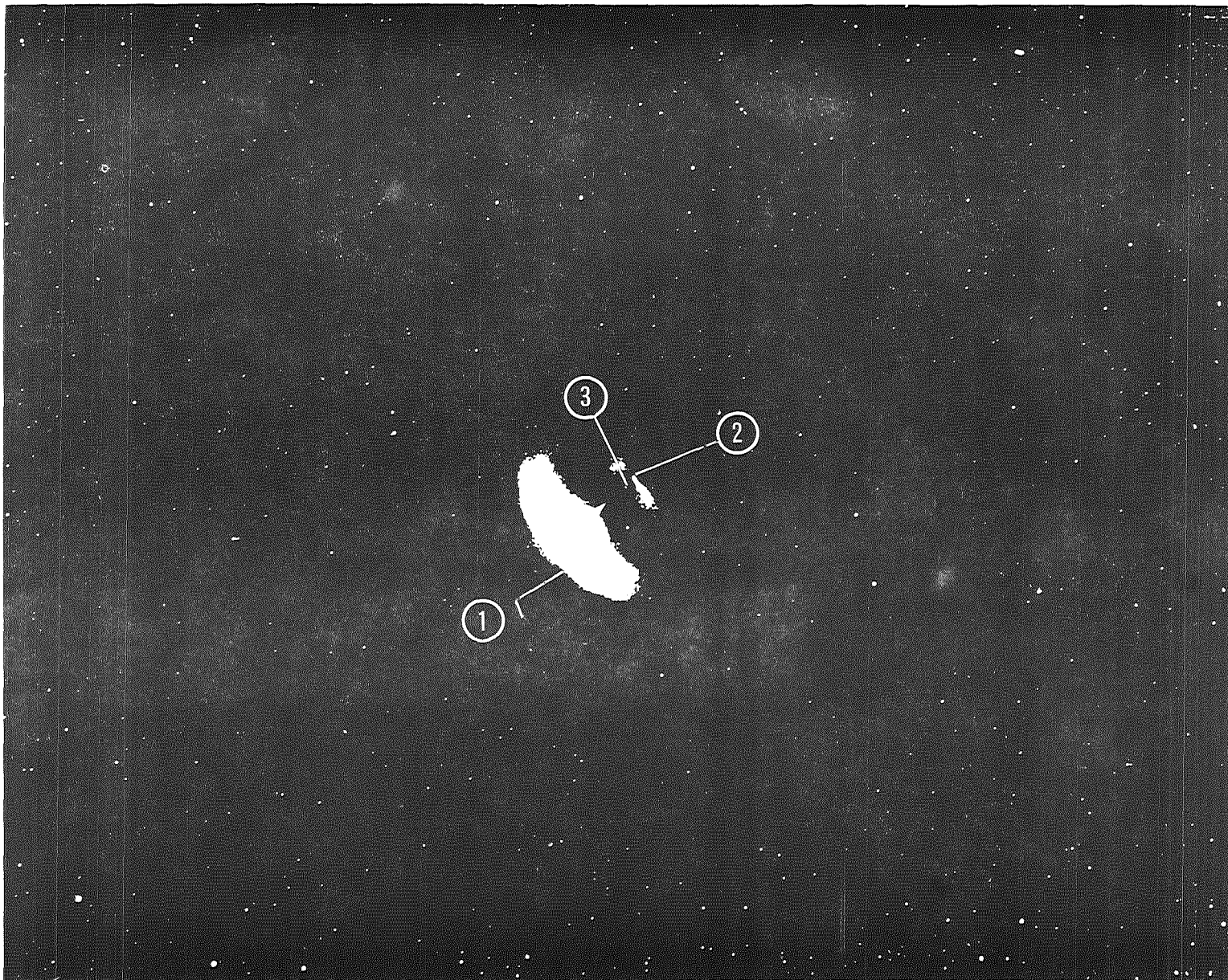


FIGURE 1. BAKER-NUNN PHOTOGRAPH OF THE APOLLO 8 LIQUID OXYGEN RELEASE. OBJECT (1) IS THE OXYGEN CLOUD, OBJECT (2) IS THE S-IVB, AND OBJECT (3) IS THE COMMAND AND SERVICE MODULE.

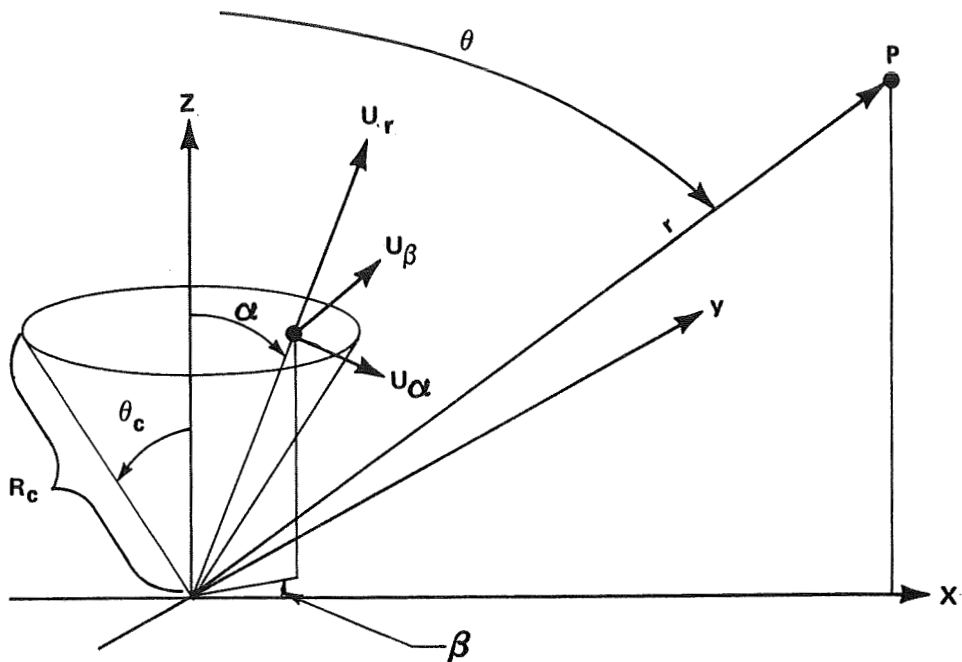


FIGURE 2. THIS SCHEMATIC SHOWS THE COORDINATE SYSTEM USED IN THIS ANALYSIS.

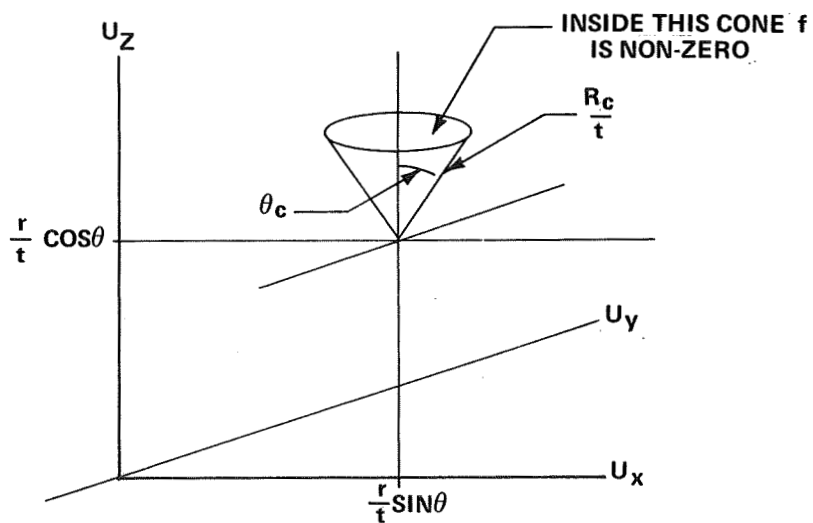


FIGURE 3. THIS SCHEMATIC SHOWS THE INTEGRATION REGION FOR EQUATION (8).

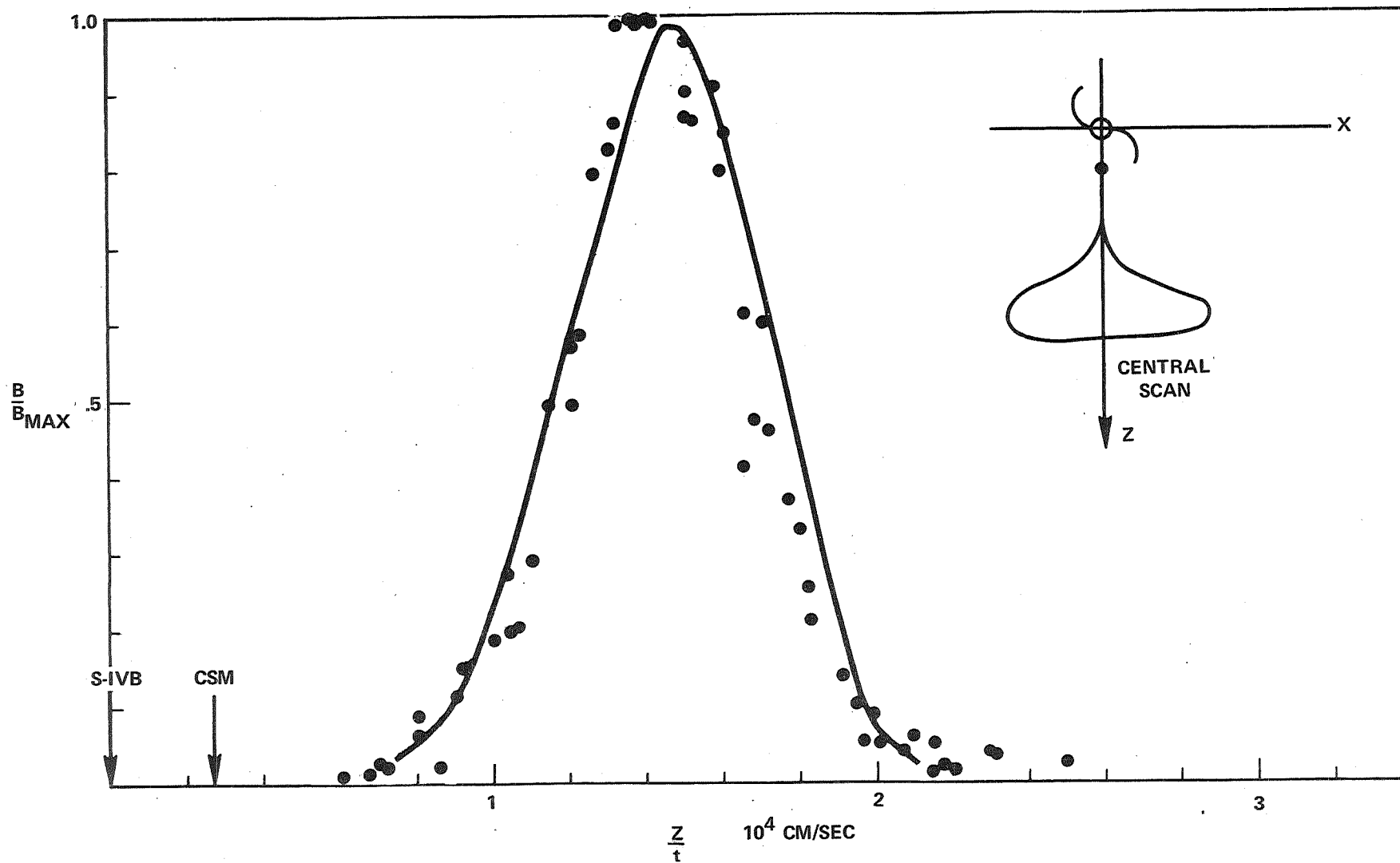


FIGURE 4. RELATIVE BRIGHTNESS ALONG THE CENTER LINE OF THE OXYGEN CLOUD.

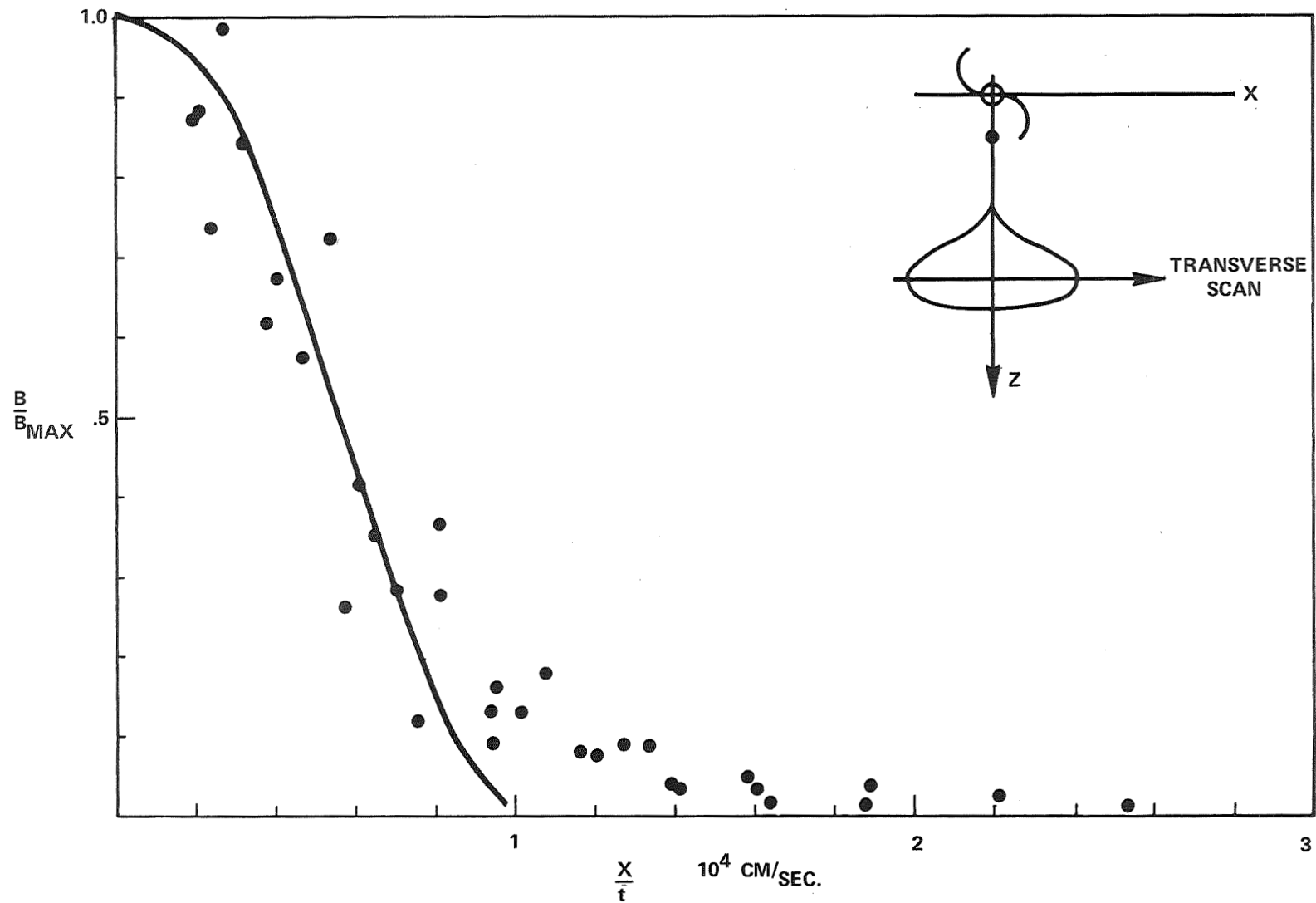


FIGURE 5. RELATIVE BRIGHTNESS ALONG A TRANSVERSE SCAN THROUGH THE POINT OF MAXIMUM BRIGHTNESS.